ELSEVIER

Dislocation avalanches: Role of temperature, grain size and strain hardening

Thiebaud Richeton *, Jérôme Weiss, François Louchet

Laboratoire de Glaciologie et Géophysique de l'Environnement, CNRS 54 rue Molière, BP 96, 38402 Saint Martin d'Hères Cedex, France

Abstract

Previous acoustic emission experiments on creeping single crystals of ice showed that the dynamics of an assembly of interacting dislocations self-organized into a scale-free pattern characterized by power law distributions of avalanche sizes. In this paper, we investigate the possible incidence of temperature and microstructure on this emerging pattern. Temperature does not modify the nature of the critical dynamics. However, it seems to modify the avalanche's relaxation owing to dislocation–phonon interactions. On the other hand, tests on polycrystals reveal the role of grain boundaries as barriers to dislocation motion hindering the emergence of the scale-free pattern, as well as the role of kinematic hardening as a polarized internal stress.
© 2005 Acta Materialia Inc. Published by Elsevier Ltd. All rights reserved.

Keywords: Acoustic emission; Dislocation dynamics; Thermally activated processes; Grain boundaries; Self-organization and patterning

1. Introduction

Within a material-dependent range of temperature and stress [1], the (visco)plastic deformation of crystalline materials involves the motion of a large number of dislocations. There are evidences that in materials with high dislocation mobility such as face-centred cubic metals, dislocation motion proceeds in a strongly intermittent manner [2]. This means that plastic deformation takes place through isolated 'bursts' in which the instantaneous strain rate may exceed the average strain rate by several orders of magnitude [2]. These bursts are transient and strongly localized episodes called dislocation avalanches [3]. The spatial heterogeneity of plastic flow was first characterized, from a static point of view, through the observation of the surface of metals which indicated that slip consists of events localized along slip bands [4]. Subsequently, fractal dislocation cell patterns

were observed [5]. Scale-invariant patterning of dislocation arrays was also obtained in numerical simulations [6]. However, a different approach to patterning has emerged in the past few years. It involves the measurement and analysis of temporal signals generated during deformation [7]. In practice, dislocation avalanches can be investigated through their influence on various physical properties that are sensitive to the density and velocity of mobile dislocations [7]. Among a few other techniques (such as the study of the electrical response or of the stress recorded during an imposed strain rate test), acoustic emission (AE) is a powerful technique for exploring the cooperative motion of dislocations [8].

Indeed dislocation avalanches generate acoustic waves whose properties can be used to characterize the avalanche properties [8]. In former works, we performed experiments on single crystals of ice Ih, a hexagonal close-packed material with a high dislocation mobility and a strong plastic anisotropy leading to a dominant slip along basal planes [9]. It was shown that the dynamics of an assembly of interacting dislocations self-organized into a scale-free pattern characterized by

intermittency [3], power law distributions of avalanche sizes [3] (that is, of AE amplitudes A_0), $P(A_0) \sim A_0^{-\tau}$, time correlations and aftershock triggering [10], as well as fractal distributions of avalanche locations and complex space–time coupling [11]. These observations are supported by both discrete dislocation dynamics [3] (DDD) and phase-field numerical models [12]. They argue for an out-of-equilibrium system close to criticality [3,13], therefore supposedly with a high degree of universality of the statistical behaviour. They question the classical ways of modelling plasticity, which use homogenization procedures. Indeed, such a scale-free intermittent pattern precludes the definition of an elementary representative volume over which a density of dislocations, an average velocity or an average strain rate can be defined.

Here, we continue our experimental exploration of dislocation avalanche phenomena in crystalline plasticity using acoustic emission. From tests performed on single crystals, the present paper will first focus on the role of temperature. In a second part, from tests performed on polycrystals, the role of grain boundaries which can notably act as barriers to dislocation motion, will be investigated through a possible modification of the scale-free, close-to-critical dislocation dynamics observed so far. Tests on polycrystals will also be used to specify the role of strain hardening. All the experiments were performed on either single crystals or polycrystals of ice Ih, considered in our study as a model material.

2. Experimental procedure

Laboratory-grown, cylindrical ($R \approx 55$ mm, $L \approx 85$ mm) ice single crystals and polycrystals were prepared from distilled, deionized, and degassed water. Single crystals grew within a cylindrical mould frozen from the bottom in about one month from a monocrystalline seed having the c axis perpendicular to the axis of growth. Then, the sample was cut at an angle, so that basal planes, which are the preferred slip planes in hexagonal ice, were inclined at the beginning of each test from 10° to 30° from the compression axis. Two methods were used to prepare polycrystals. Their average grain size $\langle d \rangle$ varied from 260 μm to 5 mm (these grain sizes are large compared to usual grain sizes of structural materials such as metals, see Fig. 1). For grain sizes larger than 0.8 mm, fragments of ice were ground and sieved under a specific size (depending of the expected average grain size). A cylindrical mould was filled with these fragments, then pumped down to 0.1 Torr to avoid bubbles, filled with water, and finally frozen from the bottom in ~24 h. In order to obtain smaller grain sizes, fine-grained ice powders were pressed into dense aggregates. For this purpose, ice powders with particles sizes <0.2 mm were put into a stainless steel moulding
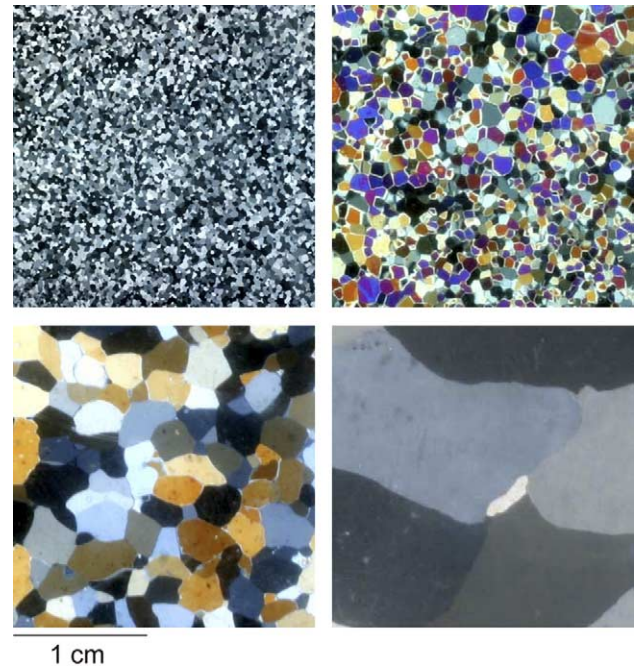

Fig. 1. Microstructures of polycrystalline ice samples. Thin sections of four ice samples with different average grain sizes observed under cross-polarized light. Top left: $\langle d \rangle = 260$ μm. Top right: $\langle d \rangle = 1.05$ mm. Bottom left: $\langle d \rangle = 1.92$ mm. Bottom right: $\langle d \rangle = 5.02$ mm.

cylinder and pressed under an axial stress of 9 MPa for a period of 2 h. This technique yielded a grain size of 260 μm which is a very small one for ice. In both cases, the c axes orientations of the grains were not controlled and so were isotropically distributed, leading to an isotropic macroscopic mechanical behaviour. The average grain sizes were determined from image analysis of thin sections and corresponded to the average of the square roots of the grain areas (Fig. 1).

As a model material to study dislocation dynamics from AE, ice provides several advantages: single crystals or polycrystals with various microstructures can be easily grown in the laboratory; transparency allows to verify that AE activity is not related to microcracking; and an excellent coupling between the ice and the AE transducer can be obtained by melting/freezing. Within the range of temperature and stress corresponding to our experimental conditions, diffusion creep is not a significant mechanism of deformation in ice, and viscoplastic deformation of hexagonal ice Ih occurs by dislocation motion [9].

Here, we only performed uniaxial compression creep experiments (constant applied stress). For the tests carried out on single crystals, we changed both the temperature and the applied stress. For the tests carried out on polycrystals with different grain sizes, the temperature was kept at −10 °C (except for one experiment performed at −3 °C), and the applied stress varied from 0.54 to 0.81 MPa, i.e., at least a factor of 2 below the threshold stress for microcrack nucleation in granular

ice [14]. The applied total deformation ranged between 6×10^{-4} and 2×10^{-3}.

During each mechanical test, one to six piezoelectric transducers responding to surface velocity with a frequency bandwidth of 200–750 kHz were fixed by melting/freezing to the side surface of the cylindrical sample. The dynamic range between the amplitude detection threshold A_{min} (3×10^{-3} V, or 30 dB) and the maximum recordable amplitude (10 V, or 100 dB) was 70 dB, i.e., 3.5 orders of magnitude. For each event detected above the threshold, the AE acquisition system allows to record different parameters (Fig. 2), among which the arrival time t_0 (the time at which the signal goes beyond A_{min}), the maximum amplitude A_0 and the avalanche duration δ. The acoustic events are individualized by the system thanks to two time constants. The first one is used to determine the time of end t_e. t_e is the time after which the signal remains below A_{min} during more than a fixed duration (100 μs in our case). Consequently, the recorded durations ($\delta = t_e - t_0$) depend on the value chosen for this time constant. The second time constant is a dead time (20 μs). A duration of 120 μs between the end of an event and the possibility of recording a new one is thus imposed. These time constants are set to avoid the individualization of secondary echoes, due to waves reflected on the sample surface. Actually, if larger than the detection threshold, secondary echoes will be included within events durations. Events durations may also include aftershocks (dislocation avalanches physically triggered by a previous one [10]). Nevertheless, once these time constants are fixed,

it is meaningful to compare from test to test the average durations of acoustic waves having a same A_0. Indeed, it provides information about how fast an avalanche damps from a same initial propagation velocity (see following section). The calibration of the experimental device was performed using a Nielsen test (a normalized artificial acoustic source).

3. AE source model

In solid materials, sudden local changes of inelastic strain generate AE waves [15]. The sources can be crack nucleation, crack propagation, twinning, or dislocation motion which is the subject of the present study. Twinning does not occur in ice, and thanks to ice transparency we verified that no crack nucleated within our samples. Moreover, in our experiments, given the amplitude threshold and the frequency range of our transducer, the detected AE are unlikely to be the result of a single moving dislocation, but are most probably related to synchronized and rapid motion of dislocations [8], the so-called dislocation avalanches. In order to interpret the characteristics of the AE waves in terms of a source mechanism, we need a model of acoustic emission source. From the theoretical analysis of Rouby et al. [16], making a low frequencies assumption ($< 10^6$ Hz) and considering the case of an acoustic transducer responding to surface velocity, one can relate the amplitude of the acoustic wave A resulting from a plastic instability, to the total dislocation length L involved in the instability and the dislocation velocity v (averaged over L):

$$A(t) = \frac{3C_T^2}{4\pi C_L} \frac{\varphi b}{D^2} Lv = \frac{3C_T^2}{4\pi C_L} \frac{\varphi b}{D^2} \left(\frac{\mathrm{d}S}{\mathrm{d}t}\right), \tag{1}$$

where C_T and C_L are, respectively, the transverse and longitudinal wave velocities, ϕ is the density of the material and D is the source/transducer distance (supposed to be large compared to L: far-field assumption). The term $1/D^2$ represents the geometrical attenuation of the acoustic waves. The term Lv accounts for the surface S swept by time unit by dislocations during the avalanche: $Lv = \mathrm{d}S/\mathrm{d}t$. When multiplied by b and normalized by a volume, this term represents a strain rate $\mathrm{d}\varepsilon/\mathrm{d}t$. An additional hypothesis is then needed to estimate the strain increment ε dissipated by the avalanche.

In this case (as in most cases where friction is involved), one can assume an exponential decay with time for the avalanche velocity, that is of the equivalent strain-rate:

$$\frac{\mathrm{d}\varepsilon}{\mathrm{d}t} = \left(\frac{\mathrm{d}\varepsilon}{\mathrm{d}t}\right)_0 \exp(-\alpha(t - t_0)) \tag{2}$$

the suffix 0 represents the onset of the avalanche at which we suppose the amplitude is maximum (in good
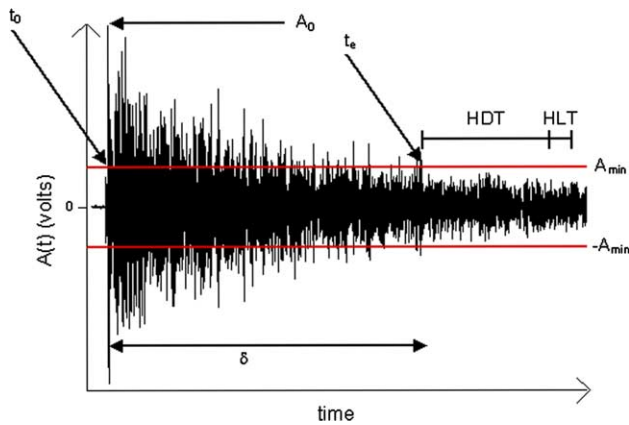

Fig. 2. Temporal acoustic wave form of a dislocation avalanche. The wave form represents the evolution of the acoustic wave amplitude A with time. The horizontal line is the detection threshold A_{min}. The AE system detects a new event as soon as $A(t)$ goes beyond A_{min} in absolute value. The first crossing corresponds to the arrival time t_0. The time of end t_e corresponds to the last crossing after which $|A(t)|$ remains below A_{min} during more than a fixed duration (HDT = 100 μs). $\delta = t_e - t_0$ is the event duration. A_0 is the maximum amplitude in absolute value of the acoustic wave on the interval $[t_0, t_e]$. At the end of the dead time (HLT = 20 μs), the system is ready to record a new event.

agreement with the wave forms recorded, see Fig. 2) and α is a damping coefficient. Then, by integrating (1) over time, we obtain a model of AE source which relates directly the value of the maximum amplitude of the acoustic wave (A_0, the parameter given by our system) to the surface swept out by dislocations during the avalanche (S):

$$A_0 = \frac{3C_T^2}{4\pi C_L} \frac{\varphi\alpha}{D^2} Sb. \tag{3}$$

Normalized by a volume, the term Sb represents a strain increment. This decay hypothesis is supported (i) by the observed decay of $A(t)$ when complete AE waves were recorded (Fig. 2), (ii) by the output of the DDD model detailed in [3] and (iii) by a good agreement between global AE activity and global deformation [8].

From this analysis, it is then also possible to relate the duration $\delta = t_e - t_0$ to the maximum amplitude of the wave, A_0. Still assuming an exponential decay for the avalanche spreading rate dS/dt, the acoustic wave amplitude at the end of an event ($t = t_e$) is:

$$A_e = A_{min} = A_0 e^{-\alpha(t_e-t_0)}, \tag{4}$$

which leads to:

$$\delta = t_e - t_0 = \frac{(\ln A_0 - \ln A_{min})}{\alpha}. \tag{5}$$

For values of A_0 smaller than 70 dB, in agreement with our exponential decay hypothesis, a $\delta \sim \ln(A_0)$ scaling is observed from our experimental data. This scaling allows to estimate the damping coefficient α. The values of α inform about the average damping of dislocation avalanches for each test. As stated previously, if larger than the detection threshold, secondary echoes and/or some aftershocks can be included within events durations. This is particularly true for large events, as the amplitudes of their secondary echoes and aftershocks are more likely to be higher than A_{min}. This may explain why we observe that the durations of large events (>70 dB) are larger than the ones that would be deduced from the $\delta \sim \ln(A_0)$ scaling.

4. Results and discussion

4.1. Effect of temperature

The individual behaviour of dislocations depends on temperature. Indeed, for instance, from −20 to −3 °C, the mobility of an individual basal dislocation in ice Ih increases by a factor of about 15 [17]. An increase of temperature may also favour the diffusion of vacancies within the crystal and consequently dislocation climb. The aim of this study was to determine whether temperature can influence the self-organization of collective dislocation dynamics. For this purpose, we performed uniaxial com-

pression creep tests on ice single crystals at −3, −10 and −20 °C. We considered three different (and arbitrary) possibilities for setting the compression stress as a function of temperature: (i) keeping the resolved shear stress on basal planes constant; (ii) keeping the macroscopic strain rate constant; and (iii) keeping the average velocity of a single dislocation constant. The idea underlying this last possibility was to maintain the behaviour of an isolated dislocation roughly the same and to see if the temperature could have an effect on their collective dynamics. In this case, we set the resolved shear stress on basal planes σ as a function of temperature T following an Arrhenius scaling, $v_i \sim \sigma \exp(-Q/kT)$ with $Q \approx 0.9$ eV [18], in order to maintain the individual dislocation velocity v_i constant.

Former work demonstrated that avalanche size distributions are independent of the applied shear stress [3], that is of the driving force for dislocation motion. The same result was obtained in the present work. In addition, it was found that whatever the method used to set the compression stress, the avalanche size distributions did not change with temperature. Indeed, once renormalized by the total number of avalanches, all the distributions collapse perfectly (Fig. 3), obeying a same power law, $P(A_0) \sim A_0^{-\tau}$, with $\tau = 2.0 \pm 0.1$. This implies that the scale-free pattern is independent of temperature. These results confirm that the scale-free critical dynamics is independent of the individual behaviour of dislocations. It results instead from long-ranged elastic interactions between dislocations, therefore exhibiting a high degree of universality. The thermally activated processes (climb, cross-slip, ...) act only on individual dislocations but do not change the critical dynamics of
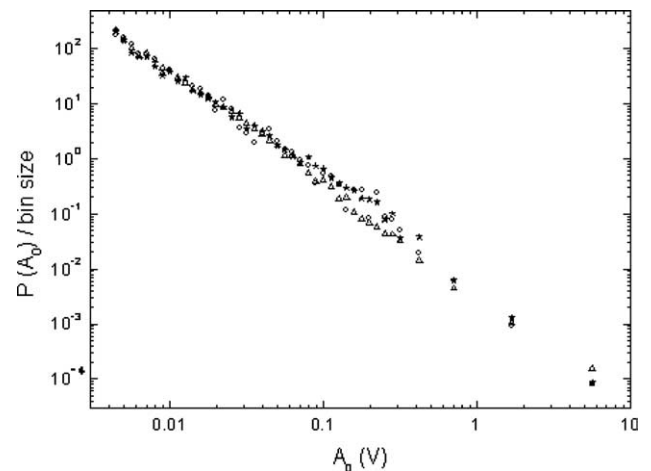

Fig. 3. Distributions of dislocation avalanche sizes in single crystals at different temperatures. Probability distributions for AE amplitudes in monocrystalline samples at different temperatures. Open circles: $T = -3$ °C; resolved shear stress on the basal planes: 67 kPa. Closed stars: $T = -10$ °C; resolved shear stress: 67 kPa. Open triangles: $T = -20$ °C; resolved shear stress: 342 kPa.

their collective motion (at least within the temperature range analyzed).

Peierls-type lattice friction opposes the glide of dislocations parallel to close-packed rows, as they have to travel through a high energy position lying between two equivalent potential troughs (see, e.g. [19]). Overcoming such a lattice friction is a thermally activated process. Lattice friction therefore increases with decreasing temperature. It also increases with strain rate, and is therefore expected to have a significant effect during fast avalanches. If strong enough compared to the average long-range interacting stress between dislocations, it may screen dislocation interactions and favour decorrelated behaviour. Consequently, the increasing part of dislocations moving in a decorrelated manner may modify the observed scale-free critical dynamics, and/or reduce the part of the global deformation taking place through dislocation avalanches. Such an effect of lattice friction was not observed, even during tests performed at −20 °C. Much lower temperatures are probably needed to observe a significant effect of lattice friction on collective dislocation dynamics in ice. Numerical simulations (in progress) might answer this question in the future. By contrast, in tests performed at the highest explored temperature (−3 °C), no 'cut-off' at high amplitudes in avalanche size distributions was observed (Fig. 3), meaning that long-range correlations remain even at a temperature very close to the melting point.

In addition to the study of the avalanche size distributions, a study of time correlations, as described in [10], was performed. A time clustering of avalanches, i.e., some aftershock activity, was systematically observed at all temperatures. The characteristics of this aftershock activity did not evolve either with temperature.

Actually, the fact that dislocation avalanche distributions are not influenced by a change of the properties of thermally activated processes is not surprising. The velocities of dislocations involved in a recorded avalanche are necessarily very high as acoustic activity is by definition related to inertial processes. In the case of very fast moving dislocations, the characteristic time scale involved in thermally activated processes may be too large for such processes to be efficient, and the lattice friction is probably overcome without the help of thermal vibrations. Accordingly, the kind of relation used to set our compression stress, which refers to thermally activated processes, probably does not apply to the case of dislocation avalanches. At very high strain rates, the predominant temperature-dependent resistance to dislocation motion is no more the overcoming of local obstacles but the drag resistance resulting from the interaction between moving dislocations and excitations, such as phonons [20]. This drag resistance occurs whatever the dislocation velocity, but can only be observed at high velocities [20]. Several experiments [20] showed that the phonon part of the drag resistance
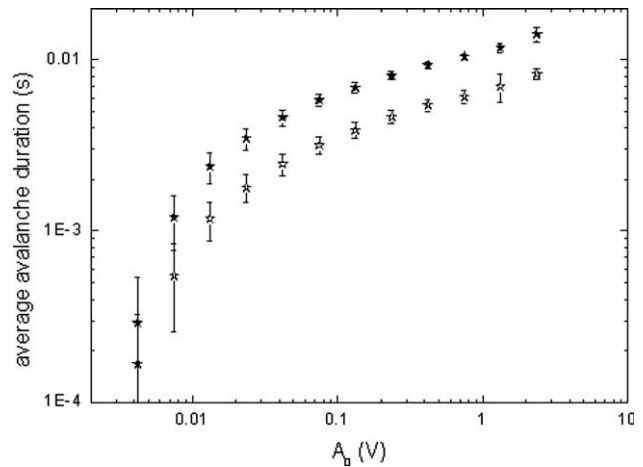

Fig. 4. Evolution of avalanche durations with temperature in single crystals. Comparison of the average duration of events of amplitude A_0 between single crystals tested at different temperatures, as a function of A_0. Closed symbols: $T = -10$ °C; resolved shear stress: 41 kPa. Open symbols: $T = -3$ °C; resolved shear stress: 67 kPa.

increases with temperature. Accordingly, in a high-velocity region, the dislocation velocity is expected to scale with temperature in the opposite way as it does in a thermally activated region. Such a difference is due to an increase of the phonon density with temperature. As mentioned above, dislocation velocities of recorded avalanches are necessarily very high. They could be high enough to observe an effect of the drag resistance on avalanches. This effect may be thus investigated through the values of the acoustic wave durations. Indeed, for a given amplitude A_0, which is from relation (1) a proxy of the initial avalanche spreading rate $(dS/dt)_0$, a shorter duration corresponds from relation (1) to a faster decrease of the dislocation velocity v with time. Actually, as we will see later, strain hardening also influences the durations of dislocation avalanches, but the tests on single crystals showed almost no hardening. Fig. 4 shows a comparison of the average duration of avalanches of the same amplitude in two single crystals tested at different temperatures. At high temperature (−3 °C), the durations δ are smaller, meaning that the average dislocation velocity v is decreasing faster. This experimental result is thus in qualitative agreement with the phonon drag resistance effect just stated.

4.2. Grain boundaries and strain hardening

The AE experiments detailed so far referred to single crystals in which complexity and multiscale properties solely arise from dislocations interacting via long-range elastic stresses. From the point of view of microstructure and dislocation motion, polycrystals, unlike single crystals, have a specific scale: the average grain size. Dislocations are indeed known to interact with grain boundaries (GBs) during plastic deformation of polycrystals in

many different ways. GBs act as strong barriers to dislocation motion, as evidenced by dislocation pile-ups that generate internal stresses (see e.g. [21] for ice). These internal stresses can activate pre-existing nearby dislocation sources in neighbouring grains [22], whereas actual dislocation transmission through GBs is possible in some specific cases [23]. GBs can also act as effective dislocation sources [24]. Accordingly, GBs acting as barriers to dislocation motion may hinder large scale propagation of dislocation avalanches, and possibly modify the scale-free, close-to-critical dislocation dynamics observed for single crystals. In order to verify this assumption, we recorded the AE during the plastic deformation of ice polycrystals with different average grain sizes, and we compared the statistical data to those obtained previously for single crystals [3].

Creep tests of ice polycrystals showed a decreasing acoustic activity as the material hardens (i.e., the visco-plastic strain-rate decreases). During stationary creep, almost no acoustic activity was recorded. The processes controlling the strain rate during this stage, such as dislocation climb in tilt boundaries (as suggested in [9]) may not be sources of AE. As a matter of fact, only transient creep, which occurs in ice essentially by basal slip [9], was a significant source of AE. Basal slip in polycrystalline samples is thus characterized by dislocation avalanches. However, the observed distributions of avalanche sizes differ from the single crystal scaling in two ways (Fig. 5): (i) the power law exponent is significantly smaller; and (ii) a cut-off of this power law scaling is observed towards large amplitudes. As for single
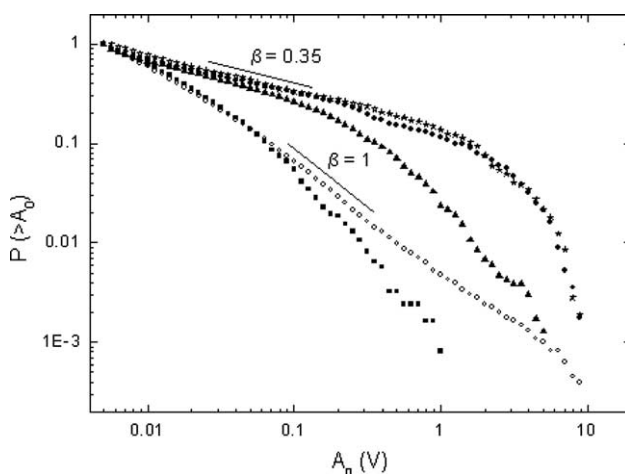

Fig. 5. Distributions of dislocation avalanche sizes in polycrystals. Cumulative probability distributions for AE amplitudes in polycrystalline samples with different average grain sizes. Closed squares: $\langle d \rangle = 0.26$ mm; $T = -10\,°C$; applied compression stress: 0.67 MPa. Closed triangles: $\langle d \rangle = 1.05$ mm; $T = -10\,°C$; applied compression stress: 0.57 MPa. Closed circles: $\langle d \rangle = 1.92$ mm; $T = -10\,°C$; applied compression stress: 0.54 MPa. Open stars: $\langle d \rangle = 1.81$ mm; $T = -3\,°C$; applied compression stress: 1.41 MPa. These distributions are compared with a typical single crystal cumulative probability distribution showing no cut-off and an exponent $\tau = \beta + 1 = 2$ (open circles).
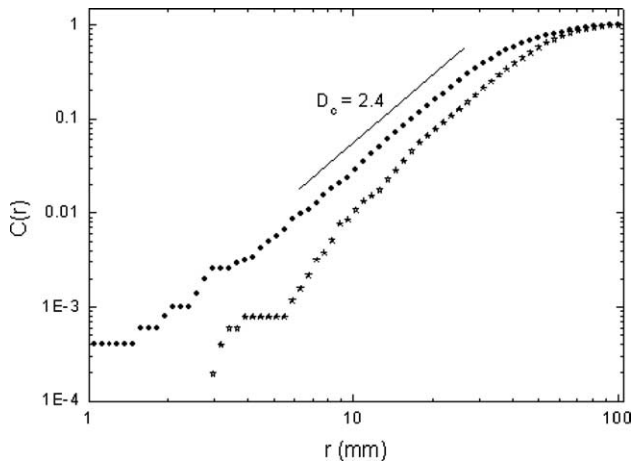
crystals, the dislocation dynamics is independent of stress level and temperature (e.g., closed circles and open stars on Fig. 5 are very close and stand for tests performed at different temperatures and stress levels but on polycrystals having roughly the same average grain size). Note that, for polycrystals, because of relatively poor statistics (between 800 and 5000 avalanches recorded for a test), a cumulative representation was preferred to better explore the high amplitudes range. We checked from Monte-Carlo simulations that this representation did not bias our estimation of the power law exponent $\tau = \beta + 1 = 1.35$, where β is the exponent of the cumulative distribution. In [25], we showed how this cut-off was linked to the average grain size of the sample. As an explanation for the change of the power law exponent, we proposed a scenario based on Monte-Carlo simulations [25]. This scenario considered that the AE waves recorded in polycrystals are related to the same deformation mechanism than in single crystals but assumed the generation of internal stresses resulting from the restraint of an avalanche by GBs. The sudden and local development of these internal stresses was then supposed to break down one of the main necessary conditions for self-organized criticality (SOC), i.e., an external driving rate much slower than the internal relaxation processes [26]. As a consequence, the system was considered as being forced to relax internal stresses through a single large aftershock into a neighbouring grain. The simulations allowed to reproduce the shape of the experimental distributions of avalanche sizes (Fig. 5): a cut-off at large scales that depends on the average grain size, as well as a decrease of the power law exponent. This scenario of aftershock triggering suggests that the localized character of plastic deformation extends towards scales much larger than the average grain size. This is supported by the result of a creep test performed on a polycrystal with $\langle d \rangle = 2.59$ mm, for which the use of 6 transducers allowed to spatially locate the avalanches in 3D. See [11] for details about AE source location. An analysis of the 3D spatial organization of the dislocation avalanches, performed by means of a correlation integral analysis (see e.g. [27] for details about this analysis), shows that avalanches are spatially correlated over distances at least one order of magnitude larger than the average grain size (Fig. 6). Indeed, within a scale range limited toward small scales by the spatial resolution threshold and toward large scales by the sample diameter (59 mm), a scale-invariant spatial distribution of avalanche locations with a correlation dimension $D_c = 2.4 \pm 0.1$ is observed.

From a macroscopic point of view, the slowing down of dislocation motion during creep tests results in a decrease of the strain rate, which means that the sample is hardening. In connection with the dislocation–GB interactions mentioned previously, polycrystals exhibit

Fig. 6. Correlation integral analysis of the avalanche locations. $C(r)$ is the probability of two locations being separated by less than r. From the data of our test ($T = -10\ °C$, applied compression stress: 0.81 MPa, $\langle d \rangle = 2.59$ mm), $C(r) \sim r^{Dc}$, with a correlation dimension $D_c = 2.4 \pm 0.1$ (closed circles). A similar analysis was performed for the same number of locations randomly distributed (a Poisson distribution) within the cylinder, which gives $D_c = 2.8 \pm 0.2$ (open stars).

significant strain hardening (Fig. 7). Hardening is either caused by the development of long-range internal stresses (kinematic hardening) and/or by short-range dislocation interactions (isotropic hardening) [9]. Polycrystalline ice shows a large contribution of kinematic hardening [9], as revealed, e.g., by a significant delayed elastic strain upon unloading of ice samples. During transient creep, the level of hardening is found to increase with decreasing grain size [28] (Fig. 7). From a microscopic point of view, the effect of strain hardening on dislocation avalanches
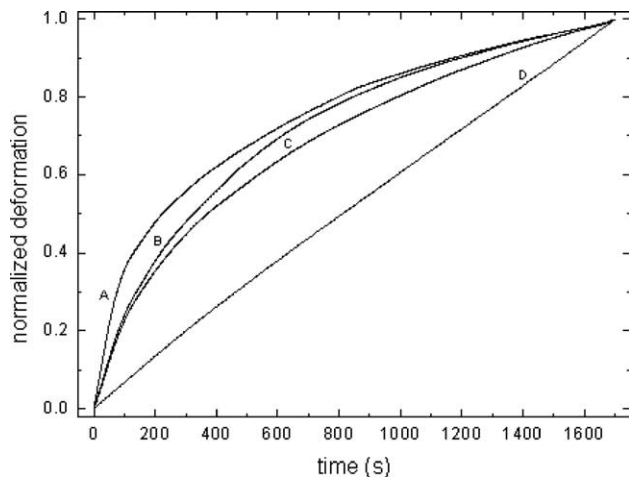

Fig. 7. Strain hardening in compression creep of polycrystals. During a creep test, the strain hardening is expressed through the decrease of the strain rate. Curve A: $\langle d \rangle = 0.26$ mm; applied compression stress: 0.67 MPa. Curve B: $\langle d \rangle = 0.87$ mm; applied compression stress: 0.54 MPa. Curve C: $\langle d \rangle = 5.02$ mm; applied compression stress: 0.55 MPa. Curve D: single crystal; applied compression stress: 0.40 MPa. All the test were performed at $-10\ °C$. As evidenced by the radius of curvature, the level of hardening increases with decreasing grain size.

may be highlighted through the values of the acoustic wave durations (as done for phonon drag resistance). Indeed, at fixed temperature and for a given amplitude A_0, a comparison of the average avalanche duration δ between different samples reveals the avalanche damping evolution with strain hardening (Fig. 8). Although the differences between the different tests are of the order of the standard deviation, a systematic tendency can be drawn: δ is, in average, smaller in polycrystals than in the single crystal (which does not harden), and δ decreases with decreasing grain size. In other words, the larger the strain hardening, the quicker the avalanches damp. This can be interpreted as a role of the back stress resulting from kinematic strain hardening on the avalanches that damp therefore more quickly. This tendency was also observed within a single test on a polycrystal: the avalanche durations were larger at the beginning of the test than at the end when the material was hardened.

Upon unloading, ice shows a reverse strain larger than the expected elastic linear strain: in connection with kinematic hardening (see above), polycrystalline ice exhibits indeed an important anelastic strain [29]. Upon unloading, a very strong but also very brief (<3 s) acoustic activity was recorded. One may assume that this acoustic activity is a consequence of the kinematic hardening: upon unloading, dislocations move back in average to their initial positions [9]. Accordingly, if dislocations start gliding back from pile-ups at boundaries, their mean free paths should be larger than upon
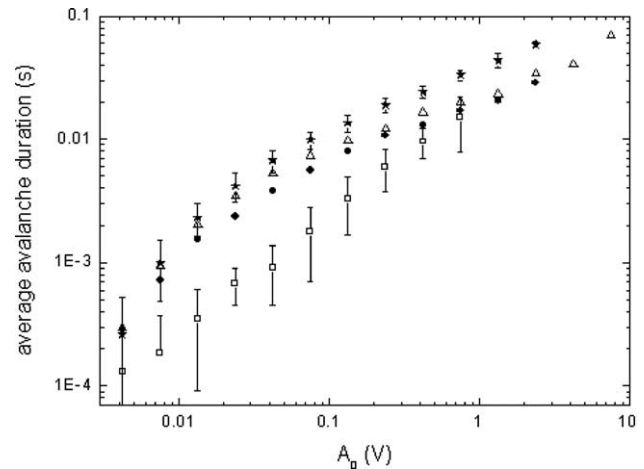

Fig. 8. Avalanche durations in polycrystals. Comparison of the average duration of events of amplitude A_0 between a single crystal and different polycrystals, as a function of A_0. Open squares: $\langle d \rangle = 0.26$ mm; applied compression stress: 0.67 MPa. Closed circles: $\langle d \rangle = 0.87$ mm; applied compression stress: 0.54 MPa. Open triangles: $\langle d \rangle = 5.02$ mm; applied compression stress: 0.55 MPa. Closed stars: single crystal; applied compression stress: 0.40 MPa. All the test were performed at $-10\ °C$. We checked that, for a given A_0, the duration data obey the central limit theorem. Therefore, averaging the durations is sensible. For a question of graph readability, error bars are only represented for the single crystal and the 0.26 mm grain size polycrystal. Otherwise error bars would overlap.

loading. This idea is consistent with the data of Fig. 9 which shows, for a same amplitude A_0, the average avalanche duration δ. As for Fig. 8, the observed differences are of the order of the standard deviation. But for avalanches larger than 0.01 V, δ is always larger upon unloading than upon loading. As expected, kinematic hardening appears as a polarized internal stress, that does not change signs upon unloading, and thus helps reverse dislocation motion. Moreover, the avalanche size distributions upon unloading show the same power law exponent as the single crystal scaling: $\tau = 2.0 \pm 0.1$ (Fig. 10). This observation argues that dislocations moving back to their initial position do not form new pile-ups at grain boundaries. Indeed, in agreement with

the scenario proposed in [25], in the absence of interactions between pile-ups of dislocations and grain boundaries, the scaling of avalanche size distributions should remain the power law scaling occurring in single crystals. However, upon unloading, no avalanche larger than 75 dB was recorded (Fig. 10). This may be a mere consequence of our limited statistics. It can also result from the fact that the total dislocation length L that can be involved in an avalanche (see relation (1)) still cannot exceed the dislocation length that can be mobilized for dislocation motion within a grain [25]. In addition, no large aftershock is expected to happen upon unloading. For all that, it is not either a question of a trivial finite size effect as, upon unloading, the spatial correlations between avalanches seem also to extend towards scales much larger than the grain size (not shown).

5. Conclusion

This paper proposed an analysis of the influence of two parameters, temperature and microstructure, on the dislocation avalanche dynamics in ice. Temperature was found to have no effect on the scale-free pattern emerging in single crystals. Nevertheless, it was possible to observe an effect of temperature on avalanche durations: the higher the temperature, the shorter the avalanche duration. This experimental observation was qualitatively interpreted by dislocation–phonon interactions. The influence of microstructure was investigated through tests on polycrystals with different average grain sizes. The introduction of a microstructural scale, the average grain size, was found to disturb the scale-free pattern observed in single crystals. However, this grain size effect was not simple, as GBs appeared to act as barriers to the dynamic propagation of avalanches but also to transmit internal stresses. More particularly, the relaxation of dislocation avalanches were influenced by GBs, as evidenced by the decrease of their durations with the level of hardening. In polycrystalline ice, reverse dislocation motion was also characterized by dislocation avalanches. But by contrast with what had been observed upon loading, the power law exponent was consistent with the single crystal scaling.

From this study, it appears that the recorded avalanche durations are influenced by both phonon drag resistance and strain hardening. This is not surprising if one considers that an avalanche experiences most of the phonon drag resistance at its onset when its velocity is maximum (hypothesis made in Eq. (2)). The importance of this drag effect against the total glide resistance would then progressively decrease as the avalanche velocity decreases. In the same time, as the avalanche moves forward, it would undergo more and more the back stresses from other dislocations present in the crystal, to finally stop.
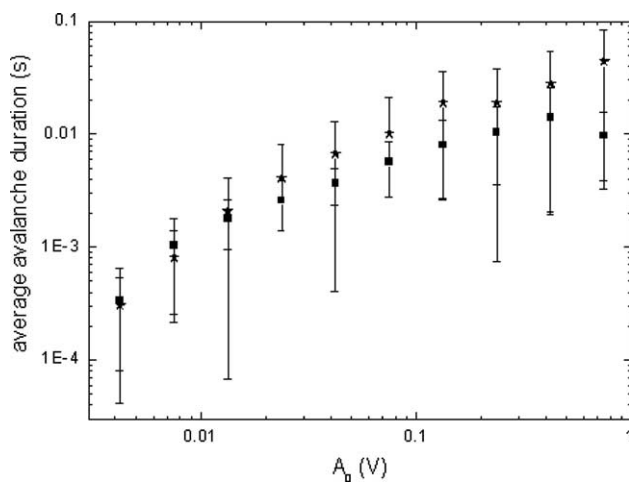

Fig. 9. Avalanche durations upon unloading. Comparison of the average duration of events of amplitude A_0 between the loading part (squares) and the unloading part (stars) of a creep test ($T = -10\ ^\circ$C, applied compression stress: 0.81 MPa) performed on a polycrystal ($\langle d \rangle = 2.59$ mm), as a function of A_0.
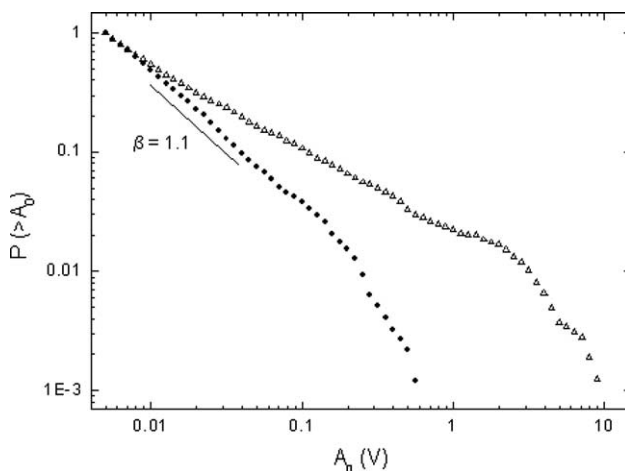

Fig. 10. Distributions of dislocation avalanche sizes upon unloading. Comparison of the cumulative probability distributions for AE amplitudes between the loading part (open triangles) and the unloading part (closed circles) of a creep test ($T = -10\ ^\circ$C, applied compression stress: 0.81 MPa) performed on a polycrystal ($\langle d \rangle = 2.59$ mm).

All these observations also challenge the modelling of polycrystalline plasticity for materials with high dislocation mobility. Indeed, the effect of GBs on dislocation avalanches proves to be very complex. Moreover, spatial correlations between avalanches extend towards scales much larger than the average grain size. Are classical micro–macro approaches such as homogenization able to deal with such a complexity? Which alternative solutions could likely deal with this problem?

References

[1] Ashby MF. A first report on deformation-mechanism maps. Acta Metall 1972;20:887–97.

[2] Zaiser M, Seeger A. In: Nabarro FRN, Duesbury MS, editors. Dislocations in solids, vol. 56. Amsterdam: Elsevier; 2002. p. 1–100.

[3] Miguel M-C, Vespignani A, Zapperi S, Weiss J, Grasso JR. Intermittent dislocation flow in viscoplastic deformation. Nature 2001;410:667–71.

[4] Neuhäuser H. In: Nabarro FRN, editor. Dislocations in solids. Amsterdam: North-Holland; 1983. p. 319–440.

[5] Hähner P, Bay K, Zaiser M. Fractal dislocation patterning during plastic deformation. Phys Rev Lett 1998;81:2470–3.

[6] Gil Sevillano J, Bouchaud E, Kubin LP. The fractal nature of gliding dislocation lines. Scripta Metall Mater 1991;25:355–60.

[7] Kubin LP, Fressengeas C, Ananthakrishna G. In: Nabarro FRN, Duesbury MS, editors. Dislocations in solids, vol. 57. Amsterdam: Elsevier; 2002. p. 101–92.

[8] Weiss J, Grasso JR. Acoustic emission in single crystals of ice. J Phys Chem B 1997;101:6113–7.

[9] Duval P, Ashby MF, Anderman I. Rate-controlling processes in the creep of polycrystalline ice. J Phys Chem 1983;87:4066–74.

[10] Weiss J, Miguel M-C. Dislocation avalanche correlations. Mater Sci Eng A 2004;387–389:292–6.

[11] Weiss J, Marsan D. Three-dimensional mapping of dislocation avalanches: clustering and space/time coupling. Science 2003;299:89–92.

[12] Koslowski M, LeSar R, Thomson R. Avalanches and scaling in plastic deformation. Phys Rev Lett 2004;93:125502.

[13] Bak P, Tang C, Wiesenfeld K. Self-organized criticality. Phys Rev A 1988;38:364–74.

[14] Frost HJ. Mechanisms of crack nucleation in ice. Eng Fract Mech 2001;68:1823–37.

[15] Malen K, Bolin L. A theoretical estimate of acoustic-emission stress amplitudes. Phys Stat Sol 1974;61:637–45.

[16] Rouby D, Fleischman P, Duvergier C. Un modèle de source d'émission acoustique pour l'analyse de l'émission continue et de l'émission par salves: I. Analyse théorique. Philos Mag A 1983;47:671–87.

[17] Petrenko VF, Whithworth RW. In: Physic of ice. Oxford: Oxford University Press; 1999.

[18] Shearwood C, Whitworth RW. The velocity of dislocations in ice. Philos Mag A 1991;64:289–302.

[19] Friedel J, Dislocations. Oxford: Pergamon Press; 1964.

[20] Nadgornyi EM. Dislocation dynamics and mechanical properties of crystals. Prog Mater Sci 1988;31.

[21] Liu F, Baker I. Dislocation–grain boundary interactions in ice crystals. Philos Mag A 1995;71:15–42.

[22] Baillin X, Pelissier J, Bacmann JJ, Jacques A, George A. Dislocation transmission through $\Sigma = 9$ symmetrical tilt boundaries in silicon and germanium I. In situ observations by synchrotron X-ray topography and high-voltage electron microscopy. Philos Mag A 1987;55:143–64.

[23] Baillin X, Pelissier J, Jacques A, George A. Direct evidence of dislocation transmission through $\Sigma = 9$ grain boundaries in germanium and silicon by in situ high-voltage electron microscopy observations. Philos Mag A 1990;61:329–62.

[24] Louchet F. In: Khan AS, editor. 7th international symposium on plasticity and its current applications. NEAT Press; 1999. p. 585–8.

[25] Richeton T, Weiss J, Louchet F. Breakdown of avalanche critical behaviour in polycrystalline plasticity. Nat Mater 2005;4:465–9.

[26] Jensen HJ. Self-organized criticality. Cambridge: Cambridge University Press; 1998.

[27] Hirata T, Satoh T, Ito K. Fractal structure of spatial distribution of microfracturing in rock. Geophys J Roy Astr Soc 1987;90:369–74.

[28] Duval P, Le Gac H. Does the permanent creep-rate of polycrystalline ice increase with crystal size? J Glaciol 1980;25.

[29] Duval D. Anelastic behaviour of polycrystalline ice. J Glaciol 1978;21:621–8.